

Why phase errors affect the electron function more than amplitude errors

Eaton Lattman^a and David DeRosier^{b*}

Received 16 October 2007

Accepted 17 December 2007

^aThomas C. Jenkins Department of Biophysics, the Johns Hopkins University, Baltimore, MD 21218, USA, and

^bRosenstiel Basic Medical Sciences Research Center and Department of Biology, Brandeis University, Waltham, MA, USA. Correspondence e-mail: derosier@brandeis.edu

If $F \exp(i\alpha)$ are the set of structure factors for a structure f , the amplitudes can be converted to those of an uncorrelated structure g (amplitude swapping) by multiplying each F by the positive number G/F . Correspondingly, the image f is convoluted with k , the Fourier transform of G/F ; k has a large peak at the origin, so that $f * k \sim f$. For swapped phases, the image f is convoluted with l , the Fourier transform of $\exp(i\Delta\alpha)$, where $\Delta\alpha$, the phase difference between F and G , is a random variable; l does not have a large peak at the origin, so that $f * l$ does not resemble f . The paper provides quantitative descriptions of these arguments.

© 2008 International Union of Crystallography
Printed in Singapore – all rights reserved

1. Introduction

Phase errors are much more damaging to the quality of the electron-density function than amplitude errors. Indeed, creating a map using the structure-factor phases from structure A and the structure-factor amplitudes from structure B gives a map in which the electron density is interpretable that from structure A (Ramachandran & Srinivasan, 1970). Similar effects have been noted in other fields (Millane & Hsiao, 2003). We present a simple way of understanding the origin of this effect.

2. The theory

Let us consider two unrelated/uncorrelated functions $f(x)$ and $g(x)$ and their Fourier transforms, $F(X) \exp[i\alpha_F(X)]$ and $G(X) \exp[i\alpha_G(X)]$, respectively:

$$f(x) = \int F(X) \exp(i\alpha_F) \exp(-2\pi i x X) dX \quad (1)$$

$$g(x) = \int G(X) \exp(i\alpha_G) \exp(-2\pi i x X) dX. \quad (2)$$

From here on we will usually leave the argument X out of equations for simplicity, and symbols such as F and G refer to amplitudes, which are always greater than or equal to zero; phases are included explicitly.

We combine the phases of G with the amplitudes of F :

$$h(x) = \int F \exp(i\alpha_G) \exp(-2\pi i x X) dX. \quad (3)$$

We can rewrite equation (3) as

$$\begin{aligned} h(x) &= \int F \frac{G}{G} \exp(i\alpha_G) \exp(-2\pi i x X) dX \\ &= \int \frac{F}{G} G \exp(i\alpha_G) \exp(-2\pi i x X) dX. \end{aligned} \quad (4)$$

We see that $h(x)$ arises from the transform of a product of two functions; one is $G \exp(i\alpha_G)$ and the other is

$$K \equiv \frac{F}{G}. \quad (5)$$

$h(x)$ is therefore a convolution of the Fourier transforms of these two functions. The transform of the first is just $g(x)$. $K(X)$ is everywhere

positive and real and is centrosymmetric. Its transform $k(x)$, therefore, is a real function with a large peak at the origin; the magnitude of the peak is given by

$$k(0) = \int K(X) dX. \quad (6)$$

The values of $k(x)$ for $x \neq 0$ are sums of both positive and negative terms with an expectation value of zero. Hence, $k(x)$ is a noisy delta function. The convolution of k and g therefore gives a noisy representation of g .

Let us now consider the function $h(x)$ in terms of $f(x)$:

$$h(x) = \int F \exp(i\alpha_F) \exp[i(\alpha_G - \alpha_F)] \exp(-2\pi i x X) dX. \quad (7)$$

Rewritten in this way, h can be viewed as a convolution of the transforms of two functions. One is the transform of $F \exp(i\alpha_F) = f(x)$. The other function is

$$L(X) = \exp[i(\alpha_G - \alpha_F)]. \quad (8)$$

The transform $l(x)$ of $L(X)$ does not have a large peak at the origin as does that of $K(X)$. Instead it has an expectation value of zero everywhere; it is simply noise without a peak. $h(x)$ is a convolution of $l(x)$ with $f(x)$ and, therefore, does not give something that resembles f at all.

3. A quantitative analysis

Let us consider the error function e_g which we define as the difference between $h(x)$ and $g(x)$:

$$\begin{aligned} e_g(x) &\equiv h(x) - g(x) \\ &= \int F \exp(i\alpha_G) \exp(-2\pi i x X) dX \\ &\quad - \int G \exp(i\alpha_G) \exp(-2\pi i x X) dX. \end{aligned} \quad (9)$$

We can rewrite this as follows:

$$e_g(x) = \int (F - G) \exp(i\alpha_G) \exp(-2\pi i x X) dX. \quad (10)$$

The r.m.s. error is simply equal to the r.m.s. value of $(F - G)$:

$$\begin{aligned} \int e_g^2(x) dx &= \int [F(X) - G(X)]^2 dX \\ &= \int F^2(X) dX + \int G^2(X) dX - 2 \int FG dX. \end{aligned} \quad (11)$$

short communications

If F and G are independent, the expected error is

$$\langle e_g^2 \rangle_{\text{exp}} = \langle F^2 \rangle + \langle G^2 \rangle - 2\langle F \rangle \langle G \rangle. \quad (12)$$

We can also predict the correlation coefficients for h with g :

$$\begin{aligned} cc_g &\equiv \int h(x)g(x) dx / \sqrt{\langle F^2 \rangle \langle G^2 \rangle} \\ &= \int dx \int F \exp(i\alpha_G) \exp(-2\pi i x X) dX \\ &\quad \times \int G \exp(i\alpha_G) \exp(-2\pi i x Y) dY / \sqrt{\langle F^2 \rangle \langle G^2 \rangle}. \end{aligned} \quad (13)$$

By integrating over x first, we obtain

$$cc_g = \int FG dX / \sqrt{\langle F^2 \rangle \langle G^2 \rangle}. \quad (14)$$

Because F and G are assumed independent,

$$cc_{g,\text{exp}} = \langle F \rangle \langle G \rangle / \sqrt{\langle F^2 \rangle \langle G^2 \rangle}. \quad (15)$$

If we now look at the difference between h and f , we get

$$\begin{aligned} e_f(x) &\equiv h(x) - f(x) \\ &= \int F \exp(i\alpha_G) \exp(-2\pi i x X) dX \\ &\quad - \int F \exp(i\alpha_F) \exp(-2\pi i x X) dX \\ &= \int F [\exp(i\alpha_G) - \exp(i\alpha_F)] \exp(-2\pi i x X) dX \end{aligned} \quad (16)$$

and

$$\begin{aligned} \int e_f^2(x) dx &= \int \int F [\exp(i\alpha_G) - \exp(i\alpha_F)] \exp(-2\pi i x X) dX \\ &\quad \times \int F [\exp(i\alpha_G) - \exp(i\alpha_F)] \exp(-2\pi i x Y) dY dx. \end{aligned} \quad (17)$$

Integrating first over x , we find

$$\begin{aligned} \langle e_f^2 \rangle &= \int F^2 [\exp(i\alpha_G) - \exp(i\alpha_F)] [\exp(-i\alpha_G) - \exp(-i\alpha_F)] \\ &\quad \times \exp(-2\pi i x X) dX \\ &= \int F^2 \{2 - \exp[i(\alpha_G - \alpha_F)] - \exp[i(\alpha_F - \alpha_G)]\} \exp(-2\pi i x X) dX. \end{aligned} \quad (18)$$

If α_F and α_G are independent,

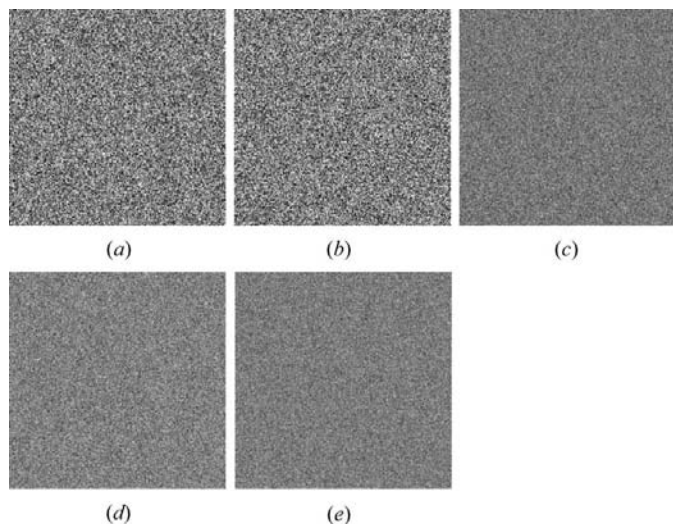


Figure 1

(a) The pseudo-random noise image corresponding to $f(x)$. The average is approximately zero and the averaged power is 1. (b) The pseudo-random noise image corresponding to $g(x)$ has an average power of 1 and an average of about 0. (c) The image h derived by applying the amplitudes derived from the Fourier transform of f to the phases of the Fourier transform of g . With careful inspection, one can see the features of g but not f in h . (d) The error function $e_f(x) = h(x) - f(x)$. (e) The error function $e_g(x) = h(x) - g(x)$.

$$\langle e_f^2 \rangle_{\text{exp}} = 2\langle F^2 \rangle. \quad (19)$$

The correlation coefficient of h and f is

$$\begin{aligned} cc_f &\equiv \int h(x)f(x) dx / \sqrt{\langle F^2 \rangle \langle F^2 \rangle} \\ &= \int dx \int F \exp(i\alpha_G) \exp(-2\pi i x X) dX \\ &\quad \times \int F \exp(i\alpha_F) \exp(-2\pi i x Y) dY / \sqrt{2\langle F^2 \rangle}. \end{aligned} \quad (20)$$

Again doing the integration over x first, we obtain:

$$cc_f = \int F^2 \exp[i(\alpha_G - \alpha_F)] dX \quad (21a)$$

because α_F and α_G are assumed independent

$$cc_{f,\text{exp}} = 0. \quad (21b)$$

By evaluating $\langle F \rangle$ and $\langle G \rangle$ using statistics, we can predict values for the r.m.s. error and the correlation coefficients. From crystallography, the probability that a Fourier coefficient has a magnitude between F and $F + dF$ is

$$P(F) dF = \frac{2F}{\sum f_j^2} \exp\left[-\frac{F^2}{\sum f_j^2}\right] dF. \quad (22)$$

We can substitute

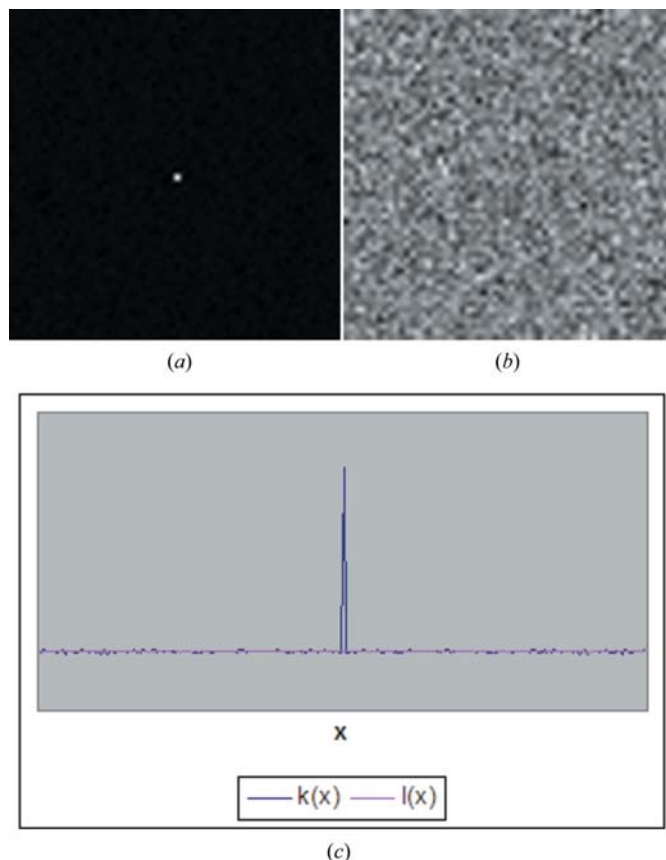
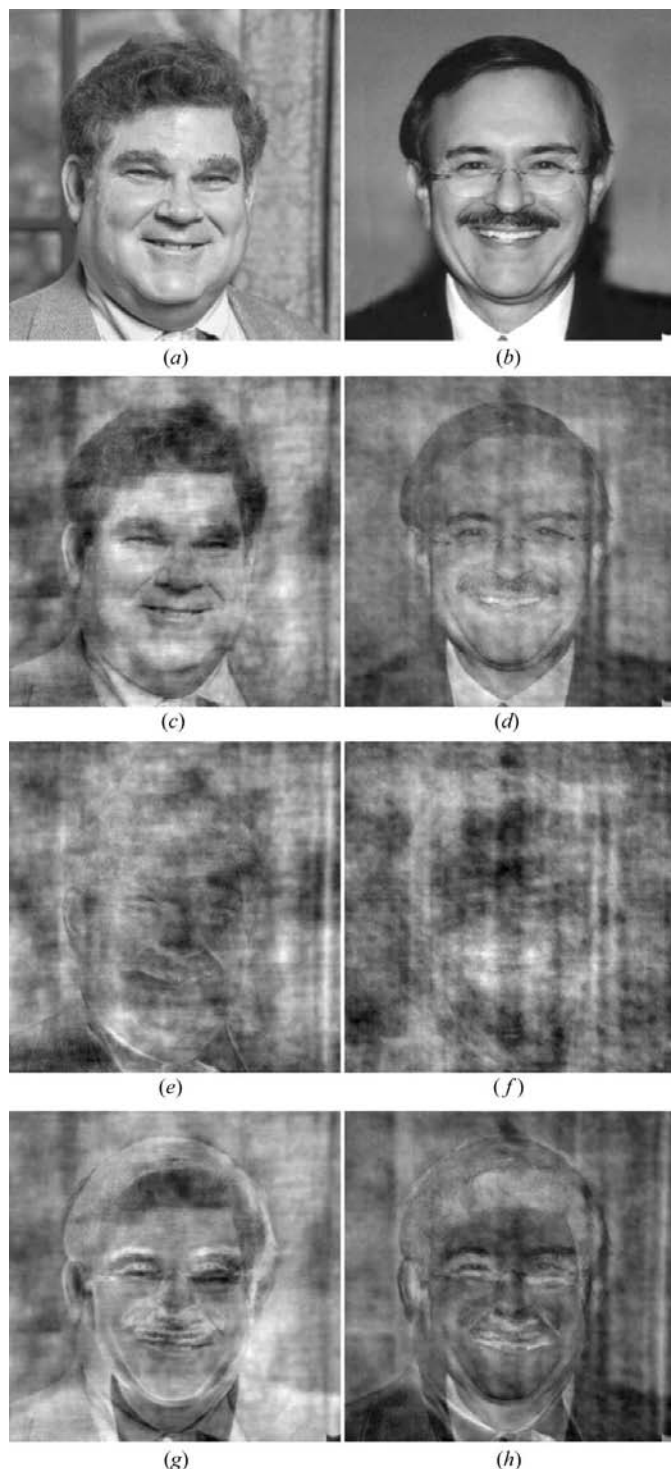


Figure 2

(a) An enlargement of the region around the origin of $k(x)$, the Fourier transform of $K(X)$, which is defined in equation (5). Note the large peak at the origin. (b) An enlargement of the region around the origin of $l(x)$, the Fourier transform of $L(X)$ as defined by equation (8). Note that there is no peak; instead it has the appearance of a noise image. (c) Line tracings of amplitude versus x taken through the images of k and l . The two curves are on the same scale. The blue curve is the trace through k and the red curve is that through l .


Figure 3

(*a*) and (*b*) are the images of the authors (EEL and DJD, respectively) with the average set to zero and the average power to 1. (*c*) The image resulting from combining the phases of the Fourier transform in (*a*) with the amplitudes from the Fourier transform of (*b*). Note that the resulting image resembles that from which the phases were obtained. (*d*) The image resulting from combining the phases of the Fourier transform in (*b*) with the amplitudes from the Fourier transform of (*a*). Note that the resulting image resembles that from which the phases were obtained. (*e*) The error map obtained by subtracting the image in (*a*) (the image providing the phases) from the image in (*c*). (*f*) The error map obtained by subtracting the image in (*b*) (the image providing the phases) from the image in (*d*). (*g*) The error map obtained by subtracting the image in (*b*) (the image supplying the amplitudes) from the image in (*c*). (*h*) The error image obtained by subtracting the image in (*a*) (the image supplying the amplitudes) from the image in (*d*). Similar figures have appeared previously (Read, 1997, p. 112).

$$\sum f_j^2 = \langle F^2 \rangle \quad (23)$$

$$P(F) dF = \frac{2F}{\langle F^2 \rangle} \exp\left[-\frac{F^2}{\langle F^2 \rangle}\right] dF \quad (24)$$

$$\begin{aligned} \langle F \rangle &= \int FP(F) dF \\ &= \int \frac{2F^2}{\langle F^2 \rangle} \exp\left[-\frac{F^2}{\langle F^2 \rangle}\right] dF \\ &= \frac{\sqrt{\pi}}{2} \sqrt{\langle F^2 \rangle} \end{aligned} \quad (25)$$

The same applies to $\langle G \rangle$, of course. If we set the powers $\langle F \rangle^2$ and $\langle G \rangle^2$ to one, we calculate that the mean squared error in $h - g$ will be

$$\langle e_g^2 \rangle_{\text{exp}} = \langle F^2 \rangle + \langle G^2 \rangle - 2\langle F \rangle \langle G \rangle = 1 + 1 - \pi/2 = 0.4290 \quad (26)$$

and the root mean squared error will be 0.65514.

The correlation coefficient will be

$$cc_{g,\text{exp}} = \langle F \rangle \langle G \rangle / \sqrt{\langle F^2 \rangle \langle G^2 \rangle} = \pi/4 = 0.78549 \quad (27)$$

The mean squared error between h and f is

$$\langle e_f^2 \rangle_{\text{exp}} = 2\langle F^2 \rangle = 2 \quad (28)$$

and the r.m.s. error is 1.414.

4. A test using images made from random noise

We tested the theory using 256 by 256 pixel images with pseudo-random white noise with the powers $\langle f^2 \rangle$ and $\langle g^2 \rangle$ set to 1 and the averages $\langle g \rangle$ and $\langle F \rangle$ are ~ 0 . The two random images, f and g , are shown in Figs. 1(*a*) and 1(*b*), respectively. The results of combining the phases of g with the amplitudes of f are shown in Table 1 and Figs. 1 and 2. The function h [equation (3)] is shown in Fig. 1(*c*), and the difference images of $h - f$ and $h - g$ are shown in Figs. 1(*d*) and 1(*e*), respectively. Figs. 2(*a*) and 2(*b*) show $k(x)$ and $l(x)$. The functions k and l when convoluted with the starting images g and f , respectively, would produce h [see equations (4), (5), (7) and (8) and surrounding text]. Note that $k(x)$ has a large peak at the origin. A trace through the peak is shown in Fig. 2(*c*). In contrast, the function $l(x)$ has no such outstanding peak, consisting primarily of noise. A trace through the origin of $l(x)$ is shown in Fig. 2(*c*); it is on the same scale as the trace shown for $k(x)$. The observed and expected values for r.m.s. error correlation coefficient are given in Table 1. The agreement, as expected, is good. The images in Fig. 1 are not particularly useful because our visual system does not easily pick out features in noise images. We therefore used more readily interpreted images.

5. A test using faces

We carried out a test using our faces as input (Figs. 3*a* and *b*). The images were 256 by 256 pixels. The average was set to zero and the power to 1. Figs. 3(*c*) and 3(*d*) show the results of putting the phases of one with the amplitudes of the other. In both cases, the face giving rise to the phases is clearly recognizable in the hybrid images rather than the one contributing the amplitudes. Figs. 3(*e*) and 3(*f*) show the difference maps between the hybrid and the image supplying the phases. Figs. 3(*g*) and 3(*h*) show the difference maps between the hybrid and the images supplying the amplitudes. Table 2 lists the observed and expected r.m.s. errors and correlation coefficients. Note that the correlation coefficients indicate that there is a correlation between the images. Indeed, the correlation coefficient is about 0.26.

Table 1

The table shows the statistics for two independent noise images.

In column 2, we computed the r.m.s. error according to equations (11) or (18) by subtraction of the transforms of the images. In column 3, we computed the correlation coefficient (cc) according to equations (14) or (21a), again using image transform values. In columns 4 and 5, we calculated $\langle F^2 \rangle$ and related values from the image transform and used them in the listed equations to calculate the r.m.s. errors and the correlation coefficients. In columns 6 and 7, we used $\langle F^2 \rangle$ and related values calculated from statistics to calculate the r.m.s. errors and the correlation coefficients.

	R.m.s. error using image transform subtraction	Correlation coefficient using image transform values	R.m.s. error using observed values	Correlation coefficient using observed values	R.m.s. error using theoretical values	Correlation coefficient using theoretical values
h with g	0.65633 square root equation (11)	0.78462 equation (14)	0.65683 square root equation (12)	0.78429 equation (15)	0.65514 square root equation (26)	0.78540 equation (27)
h with f	1.4155 square root equation (18)	-0.0019 equation (21a)	1.4142 square root equation (19)	Not done	1.414 square root equation (28)	0.00000 equation (21b)

Table 2

The table shows the statistics for the images of the authors' heads.

l refers to the image of Lattman and d to the image of DeRosier. h_l refers to the hybrid image in which the amplitudes are obtained from the image of DeRosier and the phases from that of Lattman, while h_d refers to the hybrid image in which the amplitudes are obtained from the image of Lattman and the phases from that of DeRosier. There are no values predictable by pure theory because the images are not independent; there is gross similarity between any two faces.

	R.m.s. error using image transform subtraction	Correlation coefficient using image transform values	R.m.s. error using observed values	Correlation coefficient using observed values
h_l with l	0.65759 square root equation (11)	0.78379 equation (14)	1.3868 square root equation (12)	0.05294 equation (15)
h_l with d	1.141 square root equation (18)	0.34833 equation (21a)	1.4153 square root equation (19)	Not done
h_d with d	0.65759 square root equation (11)	0.78379 equation (14)	1.3868 square root equation (12)	0.05294 equation (15)
h_d with l	1.2397 square root equation (18)	0.23152 equation (21a)	1.4346 square root equation (19)	Not done

This presumably arises because all faces are grossly similar. The predicted values for r.m.s. error and cc are in poor agreement because equations (12) and (15) assume that the input images are uncorrelated, which they are not. Because F and G are correlated, $\langle FG \rangle$ is not equal to $\langle F \rangle \langle G \rangle$; instead, the latter is smaller than the former. Hence equation (12) overestimates the r.m.s. error and equation (15) underestimates the correlation coefficient. Because F and G enter symmetrically in equations (12) and (15), we expect the values for the observed r.m.s. error and correlation coefficient in rows 1 and 3 to be identical.

We have thus shown in both qualitative and quantitative ways why phases rather than amplitudes appear to carry the essential structural information.

References

- Millane, R. P. & Hsiao, W. H. (2003). *J. Opt. Soc. Am. A*, **20**, 753–756.
 Ramachandran, G. N. & Srinivasan, R. (1970). *Fourier Methods in Crystallography*, pp. 60–71. New York: Wiley.
 Read, R. J. (1997). *Methods Enzymol.* **277**, 110–128.